



12th GLOBAL CONGRESS ON MANUFACTURING AND MANAGEMENT, GCMM 2014

## Micro-segregation studies on the Continuous Nd: YAG Laser Beam Welded AISI 316L

Arivarasu M, Vishnu G, Hari P R\*, Vipin V P, Kaushik Katiki, Gokulkumar K,  
Manikandan M, Devendranath Ramkumar K, Arivazhagan N

School of Mechanical & Building Sciences, VIT University, Vellore, Tamil Nadu, India-632014

### Abstract

This Experimental research article presents a bead on plate welding of AISI 316L welded with continuous Laser Beam Welding (LBW). An attempt is made to find a process parameter for a full penetration weld bead profile; with less segregation effect. The experiments were carried out in two sets on an AISI 316L austenitic stainless steel plate (200 x 150 x 5 mm). In the first set, trial welds were carried out by keeping the laser speed at 400 mm/min and in the second set; it was kept at 800 mm/min. In both the cases, the laser power was varied from 1000 W, 1500 W and 2000 W. Metallurgical and mechanical characterizations were carried to evaluate the weld beads. Macro and micro structural analysis is carried done to evaluate the bead profile and microstructures. Ferrite content in terms of ferrite number (FN) in the weld zone is evaluated using Fischer Feritscope. Scanning Electron Microscope (SEM)\Energy Dispersive X-ray Spectroscopy (EDS) was used to characterize the weld beads for segregation effect. Vickers micro hardness test was carried out across the cross section of the weld beads to find the hardness distribution. Better result was obtained for the trial bead with parameter 800 mm/min and 2000W.

© 2014 The Authors. Published by Elsevier Ltd. This is an open access article under the CC BY-NC-ND license (<http://creativecommons.org/licenses/by-nc-nd/3.0/>).

Selection and peer-review under responsibility of the Organizing Committee of GCMM 2014

**Keywords:** Nd: YAG laser welding; Micro-segregation; AISI 316; SEM/EDS; Ferrite Number

Nd: YAG	Neodymium-doped Yttrium Aluminium Garnet
SEM	Scanning Electron Microscope
EDS	Energy-dispersive X-ray spectroscopy
WZ	Weld Zone
WI	Weld Interface
HI	Heat Input
HAZ	Heat Affected Zone
FN	Ferrite Number

\* Corresponding author. Tel.: Phone: +9187546-89269; fax:+91416-2243092  
E-mail address: [hari.pr@vit.ac.in](mailto:hari.pr@vit.ac.in)

## 1. Introduction

Austenitic stainless steels are one of the most common and familiar types of stainless steels. 316L has low carbon which is immune to sensitization and is extensively used in heavy gauge welded components.[1] These steel structures also give excellent toughness even down to cryogenic temperatures. Compared to other chromium-nickel austenitic stainless steels, SS 316L offers higher creep, stress to rupture and tensile strength at elevated temperatures.[2] It has excellent resistance to pitting, stress corrosion cracking and acid environments. They are resistant to corrosion in various environments- ranging from room temperature to even boiling sea water.[3] The reason behind this corrosion resistance is due to the presence of a thin chromium oxide film on the surface. AISI 316L finds their application in piping, vessels, super heaters and re-heaters in oil and gas industry, refineries, chemical and petrochemical plants marine applications, architectural applications and medical implants.[4-5]. Laser welding of austenitic stainless steel has achieved a great attention in the industries because of its applications in medical implants, automotive, nuclear power plants, petroleum refineries, household etc. As AISI 316 L is a prime candidate in the aforesaid applications, studies on mechanical and metallurgical properties of laser welded AISI 316 L has found considerable amount of significance in the recent days. Proper mathematical models have to be developed for optimizing the welding process [6]. The nature of the laser beam enables it to be focused on a small spot, allowing high power density to be achieved. This advantage is the main feature in representing its potential as a welding process [7]. This technique produces good metallurgical properties, high production rate and increases automation possibilities [8]. It is well known that whatever the welding method, fusion welding generally involves heating the two joined parts together which can cause modification of the structures with loss in material characteristics. In other words the properties of weld and the area around the weld-bead (HAZ) would be affected with variation in the metallurgical and mechanical properties [9]. Manikandan et al. [10] studied the welding of alloy C-276 using the continuous Nd:YAG laser welding and concluded that the amount of micro segregation is considerably less in laser welding technique because of its rapid cooling rate.

In this experimental research work, bead on welds were carried out on AISI 316 stainless steel plates with varying the laser process parameters. The bead on studies using continuous current Nd: YAG laser beam welding on the AISI 316 were not found in the available open literature. Generally bead on studies will be carried out to find the optimum process parameters for geometrical characteristics. In this research work an attempt is made to find a process parameters not only for the full penetration weld bead profile but also to find the optimal which gives less segregation effect. The metallurgical properties like macro-micro structures, ferrite content and segregation effect. Micro segregation of the alloying element and the elemental distribution along the cross-section of the weld was examined by using SEM/EDS. Mechanical properties like depth of penetration, hardness distribution was evaluated.

## 2. Experimental Procedure

### 2.1. Candidate material and welding procedure

Candidate material for this experimental investigation is austenitic stainless steel AISI 316L of dimensions 200 x 150 x 5 mm. The chemical composition is shown in Table 1. Laser welding setup which is used for this experimentation is represented in Fig. 1. In this experimental research work, a continuous Nd:YAG laser (JK 2003SM -ABB Robot) with a spot diameter of 0.6mm was employed. Laser welding was carried out using argon as the shielding gas with a flow rate of 30 l/min and the focal length between the laser head and the work piece was maintained at 200 mm. The welding parameters were selected based on trial welds. Before welding, the plates were cleaned with emery sheets and acetone. Bead on welds were done in two sets; in the first set the speed was maintained at 400 mm/min and the power was varied from 1000W, 1500W, 2000W. In the second set, the speed was kept at 800 mm/min with power 1000W, 1500W and 2000W. The process parameters combinations employed in this experimental work is represented in Table 2. The macro structure of the weldment cross section for the different trials is represented in Fig 2.

The heat input (HI) calculation for each set of parameter was calculated using the below mentioned formulae [11]

$$HI = \frac{P}{S} \frac{J}{mm} \quad (1)$$

Where, P is the laser power in watt and S is the welding speed in mm/s.

Base Metal	Chemical Composition							
	Cr	Ni	Mn	Mo	Si	P	S	Fe
AISI 316L	16-18	10-14	2	2-3	0.75	0.045	0.03	Bal

Table. 1 Chemical composition of base metal AISI 316 L

Trial No.	Speed mm/min	Power W
1.	400	1000
2.	400	1500
3.	400	2000
4.	800	1000
5.	800	1500
6.	800	2000

Table 2. Process parameters employed for bead on welding of AISI 316L



Fig. 1 Laser Welding Setup

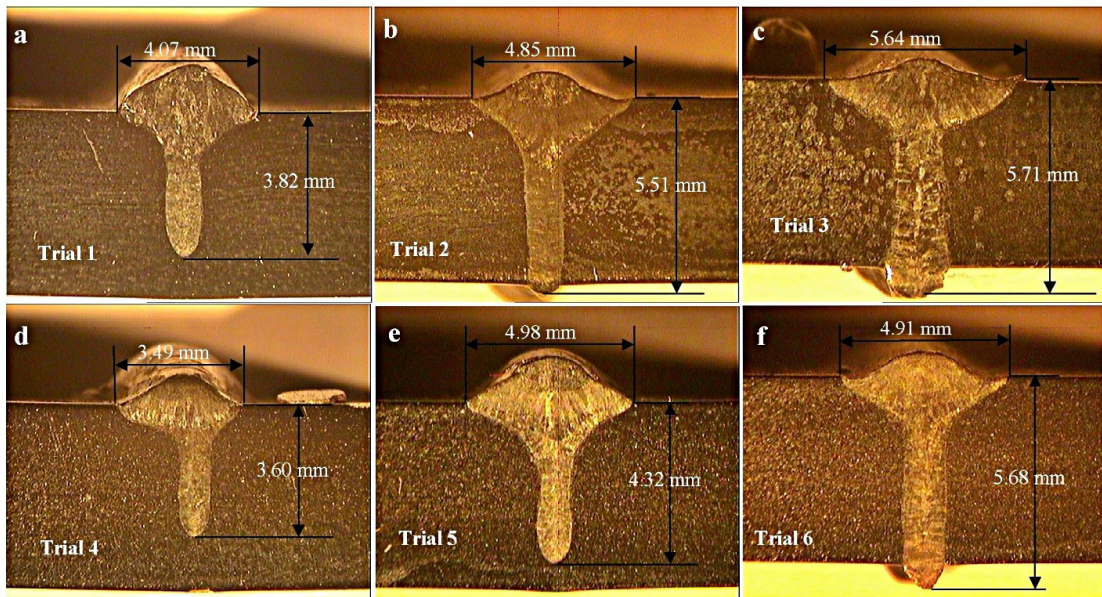


Fig. 2 Macro structure showing weld bead profile of AISI 316L at different trials

## 2.2. Characterization studies

Samples were cut from each of the weld bead to evaluate the weldment cross section for various characteristics. Both start and stop ends of the bead was discarded and the samples for macro and micro structural analysis were cut from the rest of the region by using wire Electrical Discharge Machining (EDM) technique. Standard metallographic polishing procedure as per ASTM-E3 [12] was followed. Etching of the cross sectional surface were carried out for the weld samples to obtain a better cross sectional morphology. The mixed acid etchant consisting of 15ml HCL, 10ml HNO<sub>3</sub> and 10 ml HCOO<sub>3</sub> was used to study the macro and microstructures. The macrostructure evaluation of the bead on welds was done using optical microscope. The macro examination of the cross section revealed bead profile and the depth of penetration. Microstructural analysis was done using Carl Zeiss make optical microscope respectively. These studies gave more information on the structures in the weld zone in different zones of the weld. The specimens with full penetration weld beads Trials 2, Trial 3 and Trial 6 [Fig. 2 (b, c and f)] were taken for further characterization studies. SEM/EDAX, Ferrite Number (FN). Vickers micro hardness testing was done on the weldment cross section with an interval of 0.25mm to evaluate the hardness across the weld profile.

## 3. Results and Discussion

Visual examination showed that all the beads were good and free from weld defects like crack, porosity, spatters and undercut.

### 3.1. Macrograph Analysis

Macrographs of the bead on welds are represented in Fig. 2 (a-f). Careful observation shows that the weldment is smooth and free from surface and sub surface defects like porosity, cracks, undercut and spatter. Image tool software 3.0 is used to measured bead geometry of the trial welds and is represented in Table 3. Full penetration was obtained at higher heat input trials and is evident from Fig. 2(b, c and f). Also, from the macro images it is observed that the depth of penetration is found to be decreasing as the laser scanning speed increases. From Table.3 it can be perceived that and a better penetration is achieved at lower scanning speed accompanied with higher heat input. As the laser power is increasing there is slight increase in penetration depth. However compared to welding speed, laser power has a lesser influence on the bead geometry. It is evident from that macro structure images that weld width is found to be narrow and the HAZ is found to be negligible when compared to that formed in the conventional arc welding processes.

Table. 3 Process parameters of the various weld beads, their bead geometry and their respective Heat Inputs (HI)

Trial No.	Laser power (W)	Welding speed(mm/min)	Bead Height (mm)	Bead width (mm)	Depth of penetration(mm)	Heat Input (J/mm)
1	1000	400	1.33	4.07	3.82	150.15
2	1500	400	0.70	4.85	5.51	225.25
3	2000	400	0.58	5.64	5.71	300.30
4	1000	800	0.80	3.49	3.60	75.02
5	1500	800	1.33	4.98	4.32	112.53
6	2000	800	0.63	4.91	5.68	150.04

### 3.2. Microstructural Study

The base material microstructure is shown in Fig. 3. The grain boundaries of pure austenitic phases are clearly visible. The Fig. 4-6 shows the microstructures of the bead on welded samples with different parameters. Delta ferrites were prominent in all the weld zones. Microstructure of the weld zone in trial 2 [Fig. 4(a-b)] showed comparatively lower delta ferrite content. This may be due to lower welding speed which results in lower cooling rate and formation of columnar dendritic structure [Fig. 4(a-b)].

The high laser density and power has resulted in a microstructure with a mixed but a pattern of smaller sized dendrites which can be seen from the **Fig. 5(a-b)**. It can be noticed that from lower speed to higher, amount of delta ferrite increases. The concentration of delta ferrite is found to be sparse at a welding speed of 400 mm/min [**Fig. 4(a)**]. As the speed is increased to 800 mm/min the grains become denser and the amount of delta ferrite increases as observed in **Fig. 6(a-b)**. On observing the microstructure obtained by Trial 6 [**Fig.6 (a-b)**], densely populated fine fragmented skeletal ferrite is witnessed. The possible reason for this is the faster rate of solidification due to a higher welding speed [13, 14].

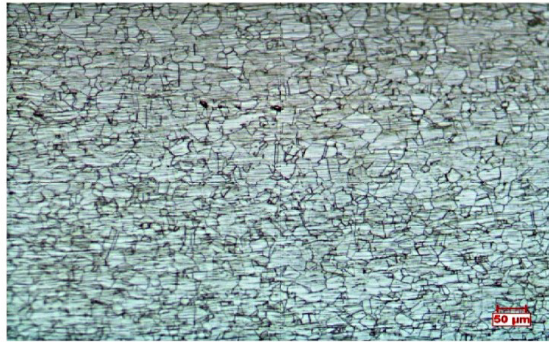


Fig. 3 Micro structure of base metal AISI 316L

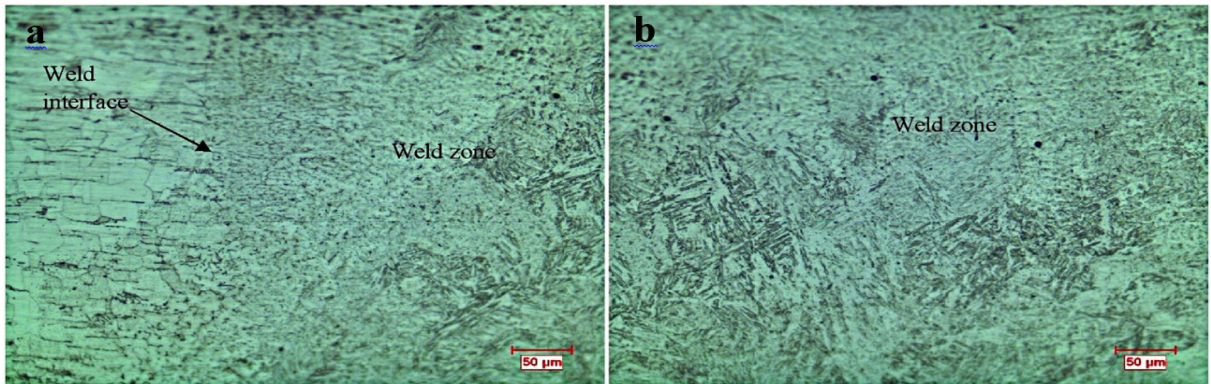


Fig. 4. (a-b) Microstructure of the bead on weld in trial 2 with the parameters 400mm/min, 1500 W

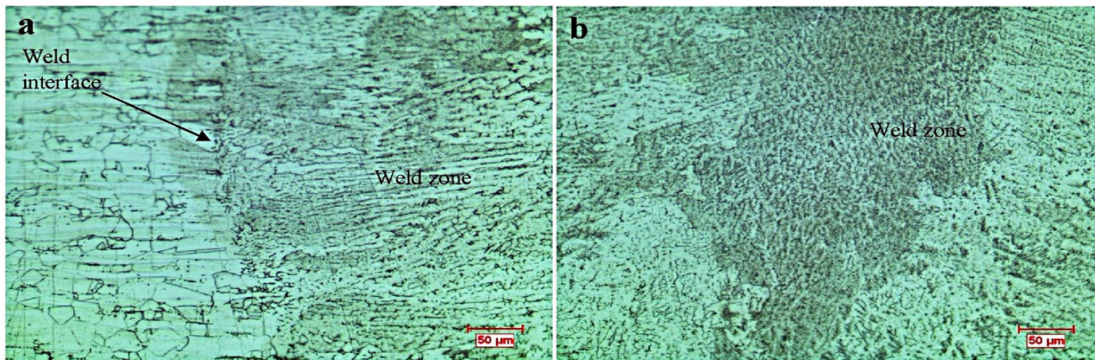


Fig. 5(a-b) Microstructure of the bead on weld in trial 3 with the parameters 400mm/min, 2000 W

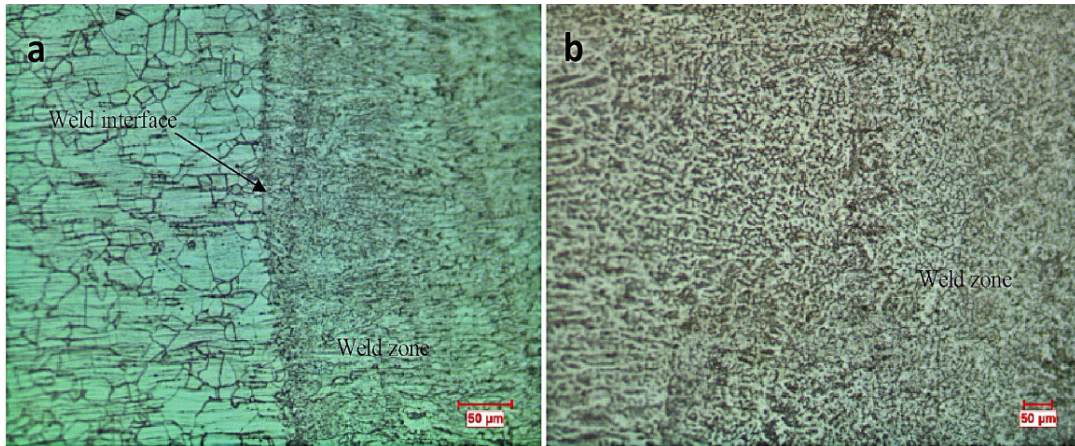


Fig. 6(a-b) Microstructure of the bead on weld in trial 6 with the parameters 800mm/min, 2000 W

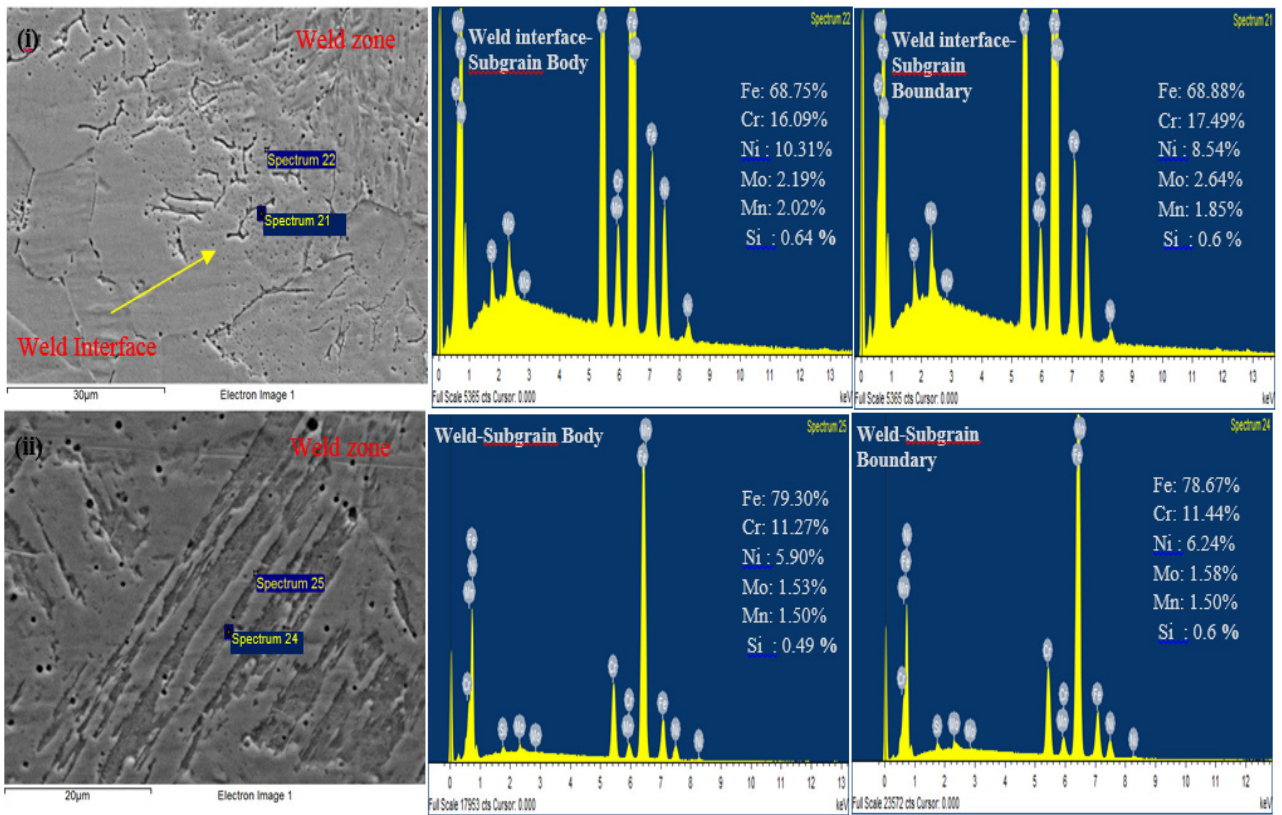


Fig. 7 SEM image and corresponding EDS analysis of the austenitic ss316L bead on weld of trial 2 at various zones.

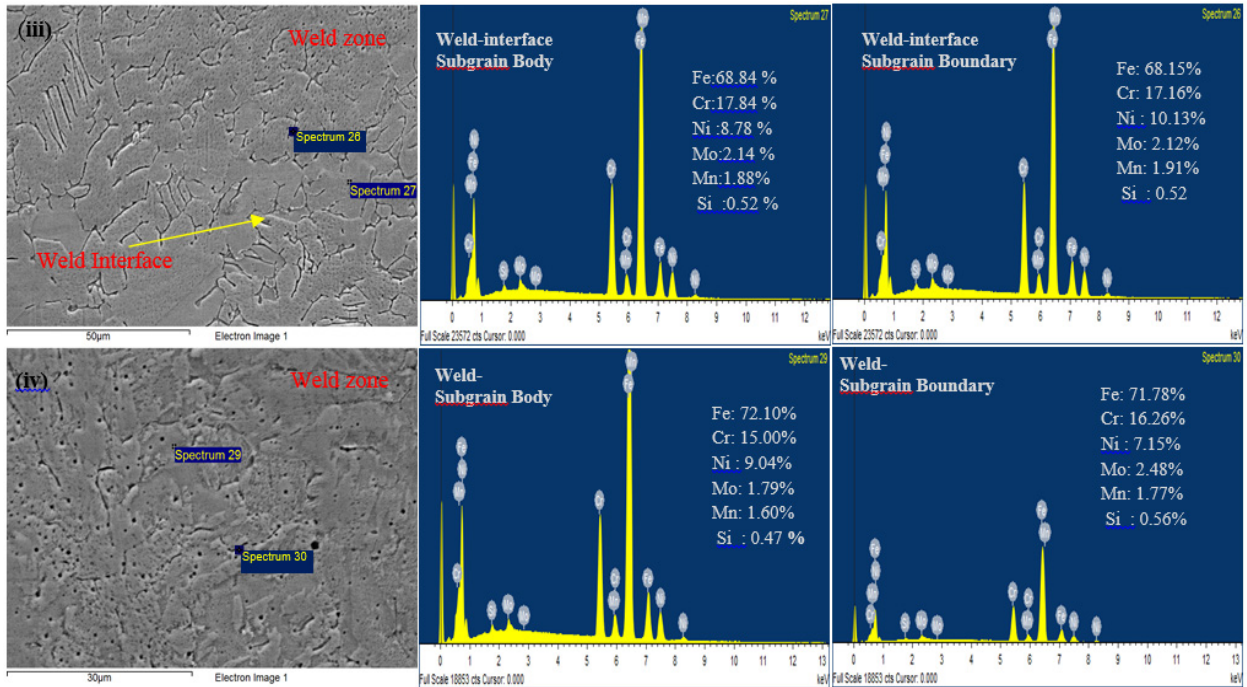


Fig. 8 SEM image and corresponding EDS analysis of the austenitic ss316L bead on weld of trial 3 at various zones.

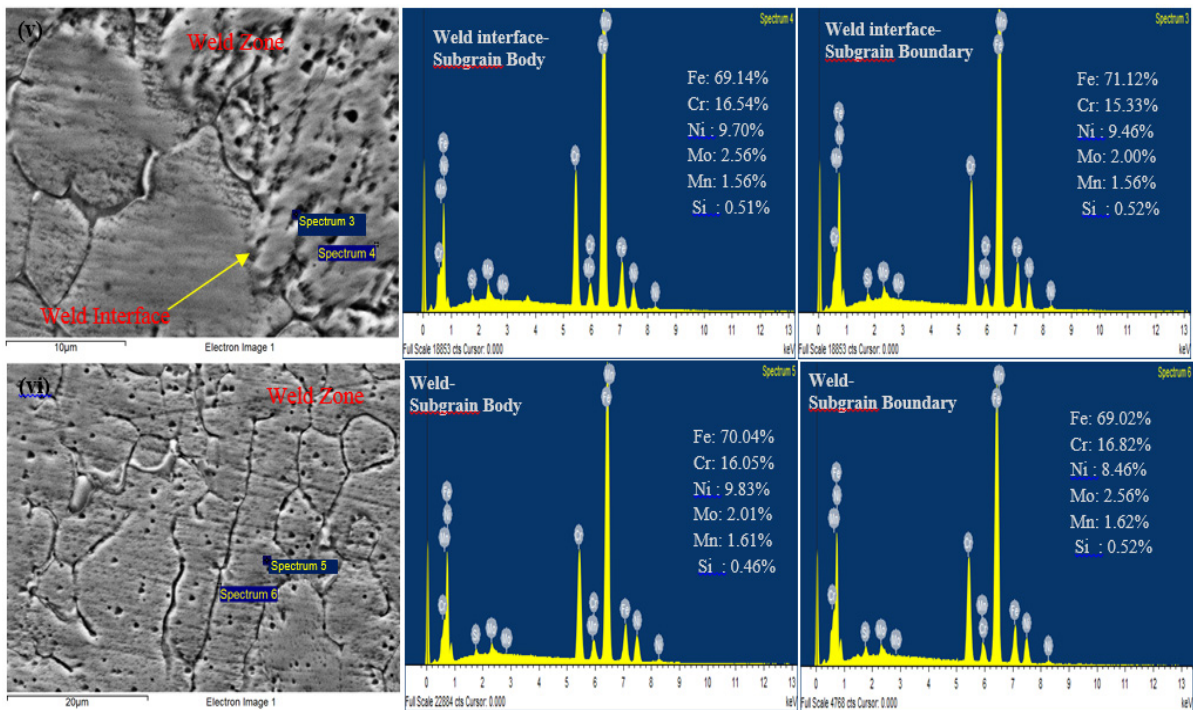


Fig. 9 SEM image and corresponding EDS analysis of the austenitic ss316L bead on weld of trial 6 at various zones.

### 3.3 SEM/EDS Analysis

The SEM/EDS analysis has been carried out along the cross section of the weldment covering the two zones weld zone (WZ) and weld interface (WI) in order to determine the effect of micro segregation across the dendritic and inter-dendritic substructure of the material. The SEM images and the elemental composition of the various trials are shown in Fig. (7-9). Elemental segregation plays a vital role in controlling the mechanical as well as the metallurgical properties of the weldments. Since the continuous Nd: YAG laser welding is used in this present study, the extent of micro segregation observed at the weld and weld interface was found to be less in all the three trials. Alloying elements at various zones for trial 2 is represented in Table. 4. On analysing these, the amount of Cr, Ni and Mo in the WZ was found to be 11.27, 5.90, 1.53 percentage respectively. These values when compared with the chemical composition of the base metal region are found to be very less. Thus, there is a difference in the chemical compositions between the weldment and the base metal in Trial 2. This may lead to a reduction in the corrosion resistance of the material. In Trial 3, [Table. 5] the amount of Ni and Mo in the WZ grain boundary was found to be 7.15 % and 2.48 %. Whereas in the WZ grain matrix the same was found to be 9.04 % and 1.79 % respectively. This may be resulted due to micro-segregation in the weld zone. Alloy composition of the Trial.6 is represented in Table. 6. The chemical composition of the Grain boundary and the grain matrix in the WI and WZ was found closer with the composition of base metal. Thus, there is very negligible segregation effect in Trial. 6.

Table. 4 EDAX elemental analyses for Trial- 2 (400 mm/min, 1500 W)

Zone	Fe	Cr	Ni	Mo	Mn	Si
Sub-grain Boundary ( WZ)	78.67	11.44	6.24	1.58	1.50	0.60
Sub-grain Body (WZ)	79.30	11.27	5.90	1.53	1.50	0.49
Sub-grain Boundary ( WI)	68.88	17.49	8.54	2.64	1.85	0.60
Sub-grain Body (WI)	68.75	16.09	10.31	2.19	2.02	0.64

Table. 5 EDAX elemental analysis for Trial-3 (400 mm/min, 2000 W)

Zone	Fe	Cr	Ni	Mo	Mn	Si
Sub-grain Boundary ( WZ)	71.78	16.26	7.15	2.48	1.77	0.56
Sub-grain Body (WZ)	72.10	15.00	9.04	1.79	1.60	0.47
Sub-grain Boundary ( WI)	68.15	17.16	10.13	2.12	1.91	0.52
Sub-grain Body (WI)	68.84	17.84	8.78	2.14	1.88	0.52

Table. 6 EDAX elemental analyses for Trial- 6 (800 mm/min, 2000 W)

Zone	Fe	Cr	Ni	Mo	Mn	Si
Sub-grain Boundary ( WZ)	69.02	16.82	9.46	2.56	1.62	0.52
Sub-grain Body (WZ)	70.04	16.05	9.83	2.01	1.61	0.46
Sub-grain Boundary ( WI)	71.12	15.33	9.46	2.00	1.56	0.52
Sub-grain Body (WI)	69.14	16.54	9.70	2.56	1.56	0.51

### 3.4 Ferrite Number (FN) Evaluation

Ferrite content present in the weld zone is measured in terms of Ferrite Number (FN) using Fischer Ferrite scope and the test results are detailed in **Table 7**. Lower ferrite number is better for corrosion resistance while balancing right amount of ferrite content avoids solidification cracking in weld deposit. The acceptable FN in the austenitic stainless steel weldment is FN 2 - 8 [13]. It can be noted from the values that either of the above mentioned properties are not affected as the values falls within the acceptable range for Trial 6. Though the welds were free from cracking in Trial 2 and Trial 3 the Ferrite Number (FN) of the same was found to slightly deviate from the acceptable range.

Table. 7 Ferrite Number (FN) at three different layers

Location	FERRITE NUMBER		
	1500 W;400 mm/min, (Trial-2)	2000 W ;400 mm/min, (Trial-3)	2000 W; 800 mm/min, (Trial-6)
Weld-Root	2.2, 2.8, 2.6	1.9, 2.0, 1.8	2.0, 2.2, 2.0
Weld-Middle	3.9, 4.6, 4.2	3.2, 2.9, 3.1	3.0, 2.9, 3.1
Weld-CAP	8.1, 9.6, 8.1	3.8, 4.6, 4.5	3.3, 3.1, 2.9

### 3.5 Vickers Micro Hardness

The micro hardness test for the full penetrated trial beads were carried out across the cross section of the weldment and are represented in **Fig. 10**. From the test results, almost similar hardness values were observed in the base metal region for all the 3 trials. In the weld interface and weld zone there is an increase in the hardness value due to the refined finer grain structure as a result of higher cooling rate involved in laser welding process [14]. The hardness value for trial 2 was found to be higher in the weld zone than the base material. Also, considerable amount of variation in the hardness is observed in this trial. The micro structure of the trial 2 shows the columnar dendrites in the austenitic matrix. The high values of hardness could be in the dendritic structure and the lower hardness values could be in the region of the austenitic matrix. The hardness value in the weld zone, with parameter 400mm/min and 2000W (trial 3) was found to be lesser when compared with the other trials. This may be due to the formation of the large amount of dispersed dendrites. The micro-hardness test results in the weld zone for the trial 6 found to be having values equal to the base material hardness also the values were found to be consistent.

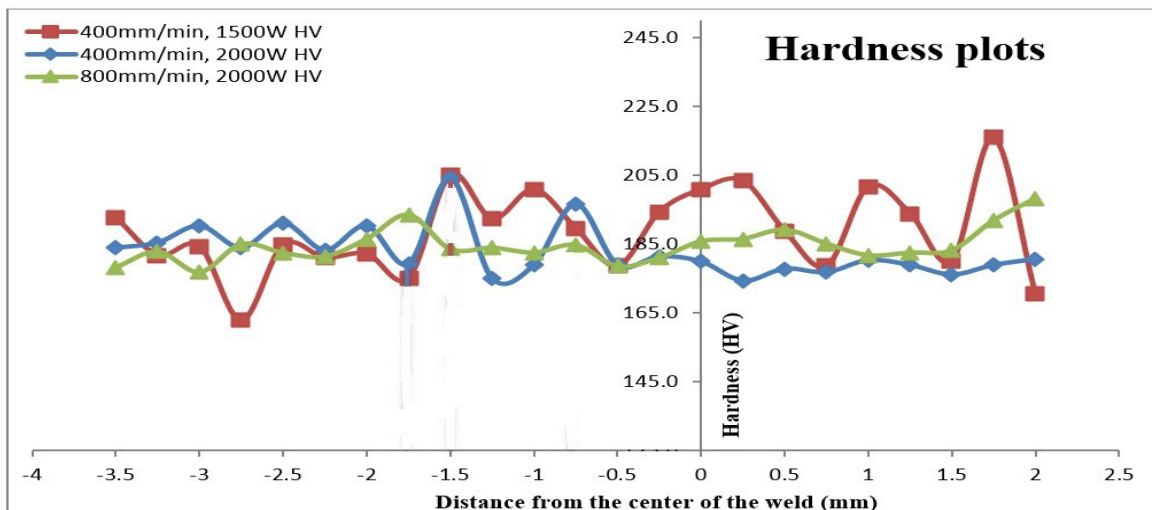


Fig. 10. Hardness profile across the weld zone of the weldments

#### 4. Conclusion

The important conclusions derived from this experimental research work are:

- a) Microstructural analysis revealed that out of six trials carried out, full Penetration weld bead is achieved in Trial 2, 3 and 6.
- b) Finer dendritic microstructure in weld metal as well as HAZ is observed at higher laser scan speeds since the rate of cooling is higher at the higher speeds.
- c) Segregation effect was found to the minimum in the Tail 6 compared to the other trials. Also the elemental composition in the weld zone and the weld interface is almost equal to the base material and hence very little or less elemental movement has occurred between the weld and the HAZ in this trial. The ferrite number values shows that corrosion resistance of the weld metal is not altered in any of the trials with full penetration.
- d) Ferrite content for the three full penetration trials was found to be Min of FN 1.9 to Max of FN 9.6. Whilst in the trial 6 it is ranging from FN 2 - FN 3.4; which divulges that the joints made with this set of parameters could be free from solidification cracking and have better metallurgical characteristics.
- e) Vickers micro- hardness results show that the weld zone hardness values of trial 6 was found to equal to the Base Material AISI 316L.
- f) As an outcome of this research work, full penetration joint of 5mm thick AISI 316L stainless steel plates with superior metallurgical and mechanical properties can be achieved in Trial 6. The recommended process parameters are; laser spot diameter 0.6 mm, focal length 0f 200mm, laser power 2000 W and laser scanning speed of 800 mm /min.

#### Acknowledgement

The authors would like to thank Department of Science and Technology for the funding received from them under the FIST programme; Laser Welding machine used in the present study was procured under this programme. The authors also like to thank the Management of VIT University, Vellore for their support and encouragement to publish this paper.

#### References:

- [1] Michael F Mcguire, Austenitic Stainless Steels Stainless Steels for Design Engineers
- [2] C.D. Lundin, Weld. J. 61 (2) (1982) 58s.
- [3] R. Viswanathan, Proc. AWS: EPRI Conf. Joining Dissimilar Metals, Pittsburg, PA (1982), pp. 7.
- [4] M. Sireeshaa, V. Shankar, Shaju K. Albert, S. Sundaresan, Microstructural features of dissimilar welds between 316LN austenitic stainless steel and alloy 800, Materials Science and Engineering, A292 (2000) 74 – 82
- [5] C.O.A.Olsson, D.Landolt, Passive films on stainless steels- chemistry, structure and growth, Electrochimica Acta, 48 (2003) 1093-1104
- [6] Cleiton Carvalho Silva, Jesualdo Pereira Farias, Hosiberto Batista de Sant’Ana, Evaluation of AISI 316L stainless steel welded plates in heavy petroleum environment, Materials and Design, 30 (2009) 1581–1587.
- [7] C. Dawes, Laser welding, Abington Publishing, New York, 1992.
- [8] J. Charles, Super Duplex Stainless Steel: Properties and Weldability, Proc. of Conference on Application of Stainless Steels, Stockholm, Jerncontoret, (1992), pp. 1108-1121.
- [9] P. Wollin, T.G.Gooch, Welding processes for stainless Steels, Welding World Journal, Vol. 36, (1995), pp. 75- 82.
- [10] M.Manikandan, P.R. Hari, G.Vishnu, M. Arivarasu, K. Devendranath Ramkumar, N. Arivazhagan, M. Nageswara Rao, G.M Reddy. Investigation of Microstructure and Mechanical Properties of Super Alloy C-276 by Continuous Nd: YAG laser Welding. Procedia Materials Science 5c (2014) 2233-2241.
- [11]Abdel-Monem, El-Batahgy, Effect of laser welding parameters on fusion zone shape and solidification structure of austenitic stainless steels, Materials Letters, 32 (1997) 155-163.
- [12] ASTM E3–11 Standard, Guide for Preparation of Metallographic Specimens, 2007, E3– 01(2007) DOI: 10.1520/E0003-11.
- [13] John C. Lippold, Damian J. Koteck, Welding Metallurgy And Weldability Of Stainless Steels, John Wiley & Sons, Inc., Hoboken, New Jersey, (2003).
- [14] P. Sathiya, S. Aravindan, P. M. Ajith, B. Arivazhagan, A. Noorul.Haq, Microstructural characteristics on bead on plate welding of AISI 904 L super austenitic stainless steel using Gas metal arc welding process, International Journal of Engineering, Science and Technology, 2(6), (2010), pp. 189-199.